# Pressure-induced superconductivity in $EuFe_2As_2$ without a quantum critical point: Magnetotransport and upper critical field measurements under high pressure

Nobuyuki Kurita,[1,2,*] Motoi Kimata,[3] Kota Kodama,[1,4] Atsushi Harada,[1] Megumi Tomita,[1] Hiroyuki S. Suzuki,[1] Takehiko Matsumoto,[1] Keizo Murata,[5] Shinya Uji,[1,2,4] and Taichi Terashima[1,2]

[1]*National Institute for Materials Science, Tsukuba, Ibaraki 305-0003, Japan*

[2]*JST, Transformative Research-Project on Iron Pnictides (TRIP), Chiyoda, Tokyo 102-0075, Japan*

[3]*Institute for Solid State Physics, The University of Tokyo, Kashiwanoha, Kashiwa, Chiba 277-8581, Japan*

[4]*Graduate School of Pure and Applied Sciences, University of Tsukuba, Ibaraki 305-0003, Japan*

[5]*Department of Physics, Graduate School of Science, Osaka City University, Osaka 558-8585, Japan*

(Received 3 August 2013; revised manuscript received 5 December 2013; published 23 December 2013)

Resistivity and Hall effect measurements of $EuFe_2As_2$ up to 3.2 GPa indicate no divergence of quasiparticle effective mass at the pressure $P_c$ where the magnetic and structural transition disappears. This is corroborated by analysis of the temperature ($T$) dependence of the upper critical field. $T$-linear resistivity is observed at pressures slightly above $P_c$. The scattering rates for both electrons and holes are shown to be approximately $T$-linear. When a field is applied, a $T^2$ dependence is recovered, indicating that the origin of the $T$-linear dependence is spin fluctuations.

DOI: 10.1103/PhysRevB.88.224510 PACS number(s): 74.25.Op, 74.25.Dw, 74.25.F−, 74.62.Fj

## I. INTRODUCTION

Since the discovery of superconductivity in LaFeAs(O, F) at $T_c = 26$ K,[1] considerable attention has been paid to iron-based superconductors (SCs) with a variety of crystal structures containing stacked iron-pnictide (or -chalcogenide) layers.[2] The maximum values of $T_c$ thus far achieved are 54–56 K (Refs. 3–5) and 39 K (Ref. 6) in the "1111" ($R$FeAsO; $R$ = rare earth) and "122" ($AFe_2As_2$; $A$ = alkaline earth or Eu) groups, respectively. Despite intensive research, the detailed mechanism of the superconductivity, for example, the symmetry of the SC order parameter, remains highly controversial.[7–12] It has been revealed that iron-based SCs have a unique Fermi surface (FS) structure, typically consisting of two- or three-hole and two-electron sheets.[13,14] The 1111 and 122 parent compounds undergo FS reconstruction associated with an antiferromagnetic (AF) order of Fe moments at $T_0$.[2] With the suppression of $T_0$ via dopings[1,6] or the application of pressure ($P$),[15] the superconducting (SC) ground state can be triggered. Hence magnetic instability may play an important role in iron-based SCs.

One of the intriguing issues of iron-based SCs is the origin of non-Fermi-liquid (NFL) behavior in their transport properties, such as $T$-linear resistivity,[16,17] which emerges as $T_0$ is suppressed. The existence of a quantum critical point (QCP), where the second-order transition temperature becomes zero, in iron-based SCs has theoretically been proposed[18] and has been demonstrated by the observation of a peak in the penetration depth, which is proportional to $(n/m^*)^{-1/2}$, at the optimal doping in the $BaFe_2(As,P)_2$ system,[19] for example ($n$ and $m^*$ are the carrier number and quasiparticle effective mass, respectively).

However, the existence of a QCP does not appear to be universal in iron-based SCs nor is its relevance to the superconductivity clear, as suggested by phase diagrams of La-based 1111 systems,[20,21] or the composition $x$ dependencies of the penetration depth and Drude weight of optical conductivity, both of which are related to $n/m^*$, in the $Ba(Fe_{1-x}Co_x)_2As_2$ system,[22,23] for example. In addition, it has been argued that the interpretation of the NFL-like behavior may not be straightforward owing to the multiband character of iron-based systems.[24,25]

Pressure tuning of the electronic structures in stoichiometric compounds is a better means of studying a QCP than tuning by chemical substitution, which might obscure a QCP by the inevitably introduced randomness. We therefore study $EuFe_2As_2$ under applied pressure (see Fig. 1). The transition temperature $T_0$ is about 190 K at ambient pressure, and the critical pressure $P_c$, where indications of the transition at $T_0$ disappear and bulk superconductivity appears, is 2.5–2.7 GPa.[26–30] This sudden disappearance of $T_0$ is incompatible with a QCP. Although the $Eu^{2+}$ moments exhibit an AF order at $T_N \sim 20$ K, the ferromagnetic (FM) alignment can be achieved at only a few teslas[31–33] and the spin disorder scattering can be minimized.[34] Because of the large exchange field from the $Eu^{2+}$ moments to the conduction electron spins, the upper critical field $B_{c2}$ for the $P$-induced superconductivity is much smaller[27,35] than that for other iron-based SCs with similar $T_c$.[36–38] These unique characteristics of $EuFe_2As_2$, thus, provide a significant opportunity to experimentally investigate the iron-based superconductivity with high $T_c$ of 30 K. Our measurements of transport properties and upper critical fields up to 3.2 GPa reported below show no evidence of diverging quasiparticle effective mass at $P_c$, indicating that the emergence of $P$-induced superconductivity in this clean system does not involve a QCP. However, it does not curtail the importance of spin fluctuations: we observe $T$-linear resistivity at pressures near $P_c$ and find that the Fermi liquid $T^2$ dependence can be recovered by the application of a magnetic field.

## II. EXPERIMENTAL DETAILS

Single crystals of $EuFe_2As_2$ were grown by the Bridgman method from a stoichiometric mixture of the constituent elements. Resistivity and Hall effect were measured simultaneously by a conventional six-contact method with an ac current $I$

 ©2013 American Physical Society

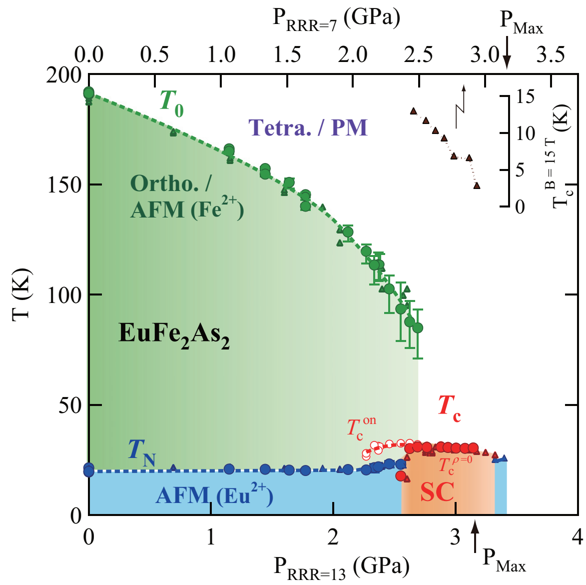


FIG. 1. (Color online) $P$-$T$ phase diagram in $EuFe_2As_2$ with $RRR = 13$ (circles, bottom axis) and 7[29] (triangles, top axis), deduced from the resistivity measurements up to 3.2 GPa under zero field. The pressure is scaled with the critical value $P_c$. PM, AFM, and SC indicate the paramagnetic, antiferromagnetic, and superconducting states, respectively. For the SC phase, open and solid symbols indicate $T_c^{on}$ (onset) and $T_c^{\rho=0}$ (zero resistivity), respectively. $T_c^{B=15\,T}$ determined at $B = 15$ T is also shown. Dashed curves are a guide to the eyes.

for $I \parallel ab$ and $B \parallel c$. For the magnetotransport measurements, we used thin platelike samples ($\sim 1 \times 0.4 \times 0.03$ mm$^3$) with residual resistivity ratio $RRR = 13$ ($P_c = 2.7$ GPa[28]). On the other hand, samples with $RRR = 7$ ($P_c = 2.5$ GPa, Ref. 29) were used to analyze the $P$ dependence of $B_{c2}$. As shown in Fig. 1, the $P$ evolutions of $T_0$, $T_N$, and $T_c$ for the two samples with different quality can be scaled by their $P_c$ values. High pressure experiments up to 3.2 GPa were performed down to 1.6 K in a $^4$He cryostat equipped with a 17 T SC magnet using a clamped piston cylinder pressure device.[39] Daphne 7474 (Idemitsu Kosan), which remains liquid up to 3.7 GPa at room temperature,[40] was used as a pressure-transmitting medium. The applied pressure was determined at 4.2 K from the change in resistance of a calibrated Manganin wire.[27] As in our previous works,[27,35] $B$ denotes the externally applied field, and the magnetization within a sample (up to $\sim$0.9 T, Ref. 34) is neglected.

## III. RESULTS AND DISCUSSIONS

First, we discuss how electron and hole carriers evolve as a function of $P$ via multicarrier analysis. Figure 2(a) shows the low-$T$ data of transverse magnetoresistivity $\rho(B)$ and Hall resistivity $\rho_H(B)$ in $EuFe_2As_2$ ($RRR = 13$) at ambient pressure. The $\rho(B)$ curves show a minimum (e.g., $\sim$2 T at 2 K), which is attributable to the $B$-induced FM alignment of the $Eu^{2+}$ moments.[31–33] At high fields, $\rho(B)$ shows positive magnetoresistance (MR), as expected from the cyclotron motion of electrons. $\rho_H(B)$ exhibits pronounced nonlinear behavior at low temperatures.[34] The field-induced transition

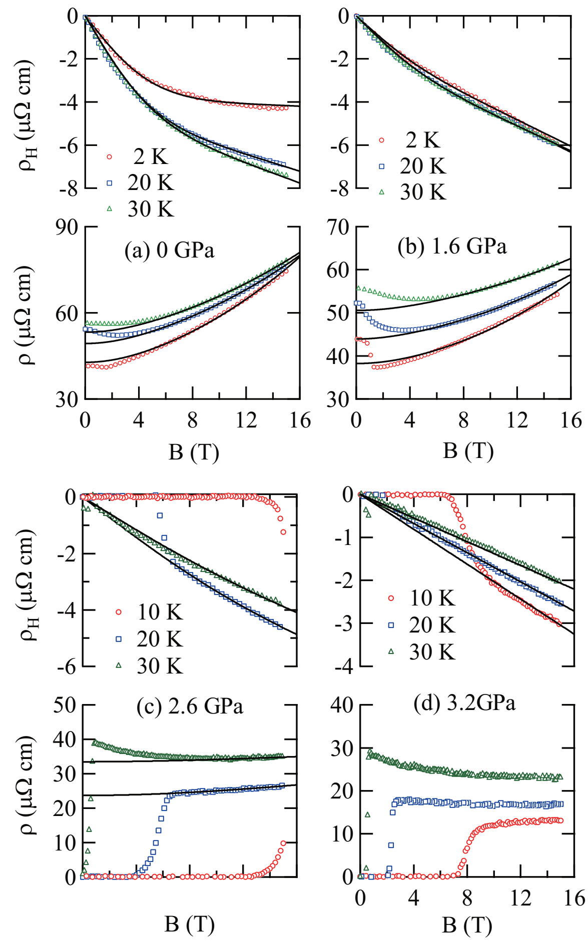


FIG. 2. (Color online) Low-temperature data of $\rho(B)$ and $\rho_H(B)$ in $EuFe_2As_2$ ($RRR = 13$) at (a) $P = 0$, (b) 1.6, (c) 2.6, and (d) 3.2 GPa. Solid curves are fits to a multicarrier model.

of the $Eu^{2+}$ moments is not detectable in the $\rho_H(B)$ curves, indicating negligible effect of the $Eu^{2+}$ moments on the number of carriers. At pressures sufficiently below $P_c$, the $\rho_H(B)$ and $\rho(B)$ curves are qualitatively similar to those at ambient pressure except that the curvature in $\rho_H(B)$ and the magnitude of MR in $\rho_H(B)$ decreases with increasing $P$ [Fig. 2(b)]. In the vicinity of $P_c$, SC transitions due to the partial [Fig. 2(c)] or bulk superconductivity appears. In the high-field normal state, $\rho(B)$ and $\rho_H(B)$ still slightly exhibit a positive MR and nonlinear behavior, respectively. As $P$ is increased to above $P_c$, $\rho_H$ exhibits nearly $B$-linear dependence [Fig. 2(d)], whereas $\rho$ indicates negative MR due to the suppression of spin fluctuations of the Fe ions,[34] except in the low-$T$ and high-$B$ regions where the cyclotron motion dominates.

Figure 3 shows the $T$ dependence of the Hall coefficient $R_H$, as defined by $d\rho_H/dB$ at $B = 0$, under several pressures.[41] The enhancement of $|R_H(T)|$ below $T_0$ for $P < P_c$ indicates the destruction of substantial parts of the FS.[34] For $P > P_c$ (inset), $|R_H(T)|$ still increases below $\sim$80 K. Similar enhancement of $|R_H(T)|$ has been observed in the paramagnetic phase of $BaFe_2(As,P)_2$, and it has been argued that the behavior cannot be explained by a multiband picture for a Fermi liquid.[42] However, in the present case, $|R_H|$ at 2.8 GPa is $2 \times 10^{-9}$ m$^3$/C

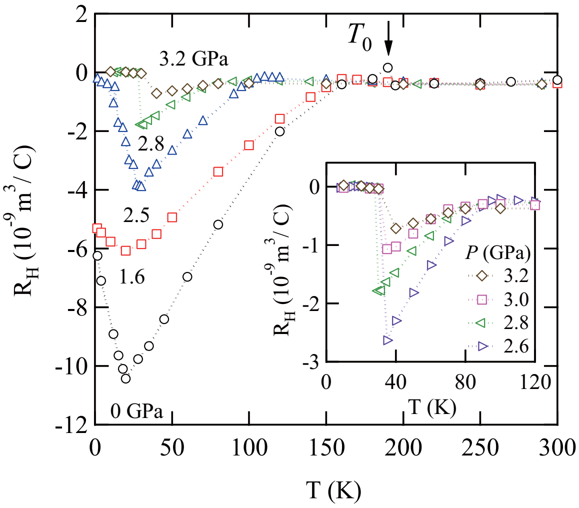


FIG. 3. (Color online) $T$ dependence of the Hall coefficient $R_H$ ($=d\rho_{xy}/dB|_{B\to 0}$) at several pressures. The inset shows an expanded view of $R_H(T)$ in the low-$T$ region at high pressures.

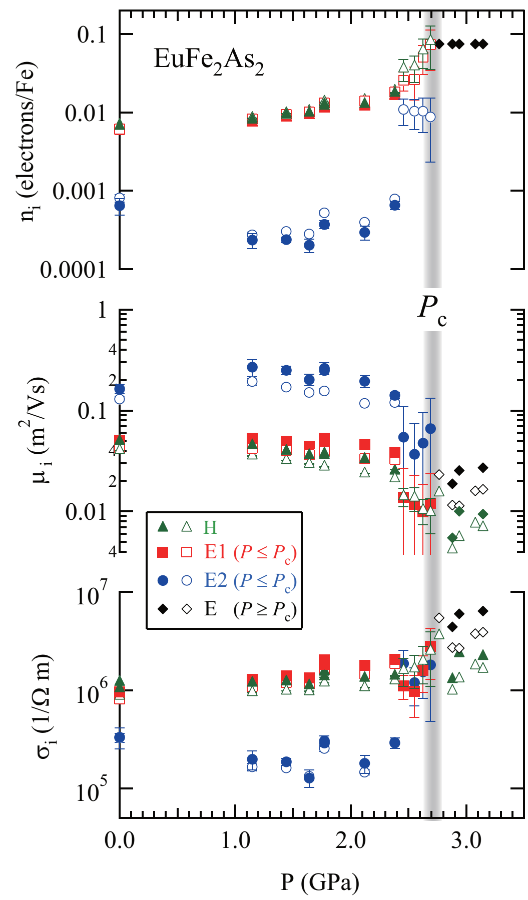


FIG. 4. (Color online) Pressure evolution of the carrier density $n_i$, mobility $\mu_i$, and conductivity $\sigma_i$, deduced from multicarrier analysis. Solid and open symbols correspond to the results obtained at $\leqslant$10 and 20 K, respectively. One hole (H) and two types of electrons (E1 and E2) are considered for $P \leqslant P_c$ (=2.7 GPa), whereas a simple two-band model with $n_H = n_E = 7.5 \times 10^{-2}$ electrons/Fe (e/Fe) is assumed for $P > P_c$.

($T \sim T_c$), which corresponds to $\approx$0.16 electron/Fe (e/Fe) in a single-carrier model. This value is comparable to the band-calculation value for $BaFe_2As_2$ (0.15 e/Fe), and hence can be accounted for within a simple two-carrier picture.

$EuFe_2As_2$ is a compensated metal with an equal number of electrons and holes, for which a simple two-carrier model predicts a linear $\rho_H$. The nonlinearity in $\rho_H(B)$ below $P_c$ thus indicates that more than two carriers contribute to the electronic transport. In the case of the sister compound $BaFe_2As_2$, a Shubnikov-de Haas oscillation study has shown that the Fermi surface in the AF phase consists of one hole and two electron pockets.[43] In keeping with this, a three-carrier model can account for the nonlinear behavior of $\rho_H(B)$ as well as the $\rho(B)$ data for $BaFe_2As_2$.[44]

We therefore apply essentially the same three-carrier analysis to the obtained $\rho_H(B)$ and $\rho(B)$ data for $EuFe_2As_2$ at $P \leqslant P_c$, assuming one hole (H) and two electrons (E1 and E2) with density $n_i$ and mobility $\mu_i$. We impose a constraint $n_H = n_{E1} + n_{E2}$, owing to the carrier compensation, which is held under applied pressures. To avoid the effect of the $Eu^{2+}$ moments or superconductivity, high-field data are used for the analysis. The solid curves in Fig. 2(a) indicate the fits, which capture the overall features of the experimental results. The fitting gives ($n_H$, $n_{E1}$, $n_{E2}$; $\mu_H$, $\mu_{E1}$, $\mu_{E2}$) = (6.6, 5.6, 0.92 [$10^{-2}$ e/Fe]; 0.57, 0.57, 1.5 [$10^3$ cm$^2$/V s]) for $T = 2$ K. The fitting errors are approximately 3% for H and E1, and 20% for E2. The parameter sets obtained at 20 and 30 K are comparable to those at 2 K. One can find the tendency that $n_H \approx n_{E1} \gg n_{E2}$ and $\mu_H \approx \mu_{E1} \ll \mu_{E2}$, similar to the case of $BaFe_2As_2$.[44] The magnitudes of the parameter sets, particularly $\mu_i$, for $EuFe_2As_2$ ($RRR = 13$) are comparable to those for as-grown samples of $BaFe_2As_2$.[44] For other pressures, a similar quality of fitting can be obtained.

At $P > P_c$, we assume one electron carrier (E) and one hole carrier (H) with $n_H = n_E$. In the analysis, the slope of $\rho_H(B)$ and the $\rho$ value at $B = 0$ are used. To determine the parameter sets ($n_H$,$n_E$; $\mu_H$, $\mu_E$) uniquely, we fix $n_H = n_E = 7.5 \times 10^{-2}$ e/Fe. A band-structure calculation suggests that the carrier density for $BaFe_2As_2$ is 0.15 e/Fe.[24] However, the shrinking of the FS has been observed in $BaFe_2(As,P)_2$[45] and has been theoretically attributed to strong interband scattering.[46] The volume of the FS is approximately halved as the optimal doping is approached in $BaFe_2(As,P)_2$.[45] We therefore use the halved value.

Figure 4 displays the $P$ evolutions of $n_i$, $|\mu_i|$, and conductivity $\sigma_i$. As the pressure approaches $P_c$, $n_i$ increases, while $|\mu_i|$ decreases. It appears that $n_i$ and $|\mu_i|$ develop reasonably continuously to their values at $P > P_c$. Neither of the $P$ dependencies of $\mu_i$ ($=e\tau_i/m_i^*$) or $\sigma$ ($=e^2\tau_i n_i/m_i^*$) suggests the divergence of $m^*$ or $(n/m^*)^{-1}$ at $P_c$.

We further substantiate the absence of a QCP by deriving the $P$ dependence of the effective masses from $B_{c2}$-$T_c$ phase diagrams under applied pressures. Figures 5(a) and 5(b) show $\rho$ vs $T$ at 2.6 and 3.0 GPa, respectively, in the $RRR = 7$ sample under several $B$ for $B \parallel ab$. $T_c$ under each magnetic field is determined by the midpoint temperature of the SC transitions. Figure 5(c) shows the thus determined upper critical field $B_{c2}$ as a function of temperature for several pressures. It appears that $B_{c2}(0)$ is highest at $P \sim P_c$ and decreases with

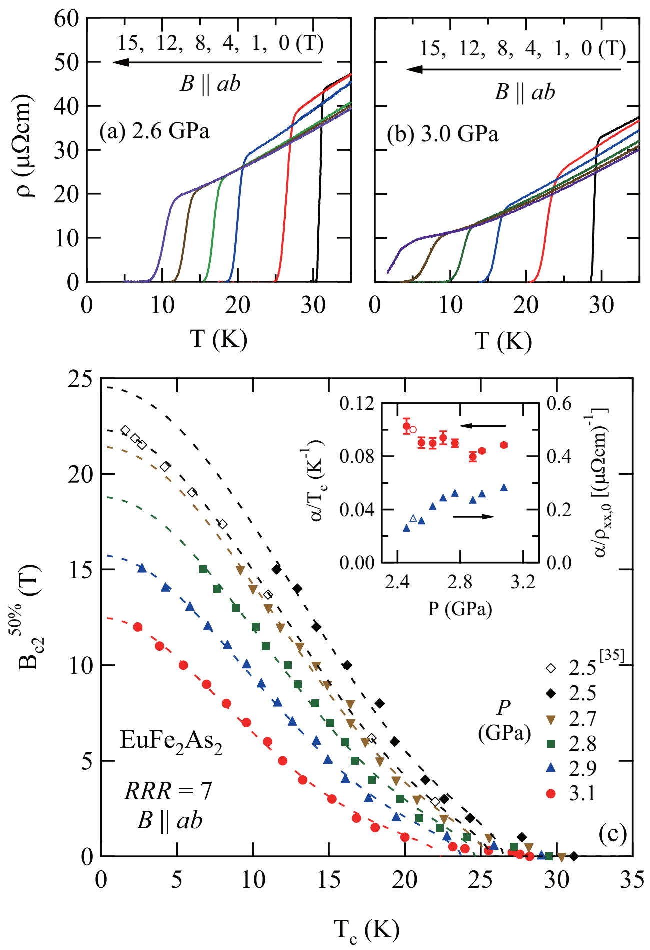


FIG. 5. (Color online) $\rho$ vs $T$ of $EuFe_2As_2$ ($RRR = 7$, $P_c = 2.5$ GPa), under several $B$ for $B \parallel ab$ at (a) $P = 2.6$ and (b) 3.0 GPa. (c) $P$ dependence of $B_{c2}^{50\%}$ vs $T_c$ of $EuFe_2As_2$ for $B \parallel ab$. Dashed curves are fits to the multiple pair-breaking formula (see text). Open symbols indicate the published data obtained from high-field resistivity measurements at 2.5 GPa up to 27 T.[35] The inset shows $\alpha/T_c$ and $\alpha/\rho_0$ as functions of $P$.

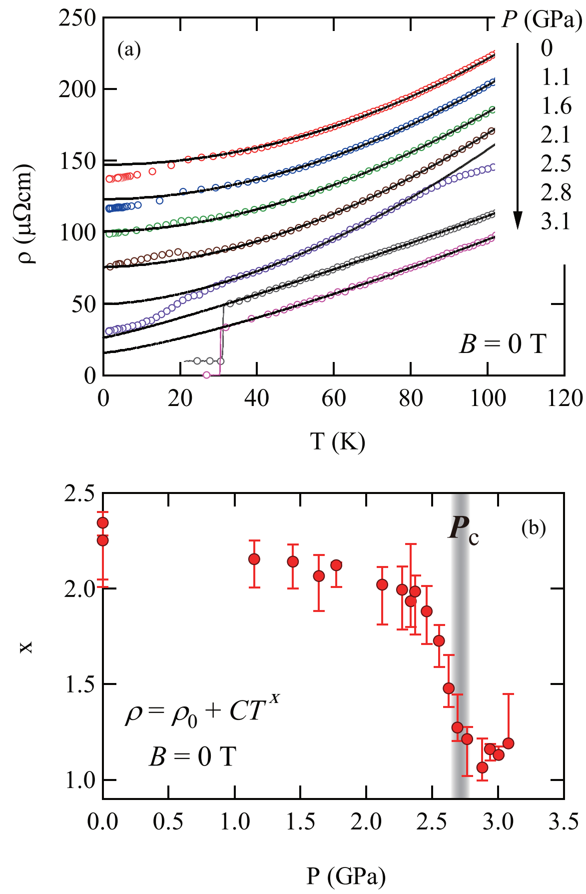


FIG. 6. (Color online) (a) $\rho$ vs $T$ under zero field at several pressures. The data are arbitrarily shifted in the longitudinal direction for clarity. Solid curves are fits to $\rho = \rho_0 + CT^x$. (b) $P$ evolution of the exponent $x$ under zero field. Solid symbols are obtained from fits in the $T$ range between 35 and 60 K. Error bars are estimated from fits in several $T$ ranges from 35 K ($>T_N, T_c$) to temperatures between 50 K and $T_0$.

increasing $P$. In $EuFe_2As_2$, orbital and Pauli paramagnetic effects and magnetic $Eu^{2+}$ moments all play an important role in determining $B_{c2}$, which complicates the understanding of the obtained $B_{c2}$ vs $T_c$. In a previous paper, we analyzed $B_{c2}(T)$ data obtained at 2.5 GPa [also shown in Fig. 5(c)] using a multiple pair-breaking model[47,48] that includes the antiferromagnetic exchange field $B_J$ due to magnetic $Eu^{2+}$ moments. We obtained the spin-orbit scattering parameter $\lambda_{so} = 2.4$, and the maximum of $|B_J|$ as $B_J^m = 75$ T, where the Maki parameter $\alpha = 3$ is fixed.[35] It is known that $m^*$ is related to $\alpha$ through $m^* \propto \sqrt{\alpha/T_c}$ or $\propto \alpha/\rho_0$ ($\rho_0$: residual resistivity) in the clean or dirty limit, respectively. Thus we estimate $\alpha$ as a function of $P$ using the same model. As $\alpha$ is highly sensitive to other fitting parameters, we use the values of $\lambda_{so} = 2.4$ and $B_J^m = 75$ T for all the pressures. Dashed curves are fitting results using $\alpha$ and $T_c$ as free parameters. The inset of Fig. 5(c) shows the $P$ dependencies of $\alpha/T_c$ and $\alpha/\rho_0$. The former exhibits only a modest increase, whereas the latter exhibits a decrease as $P_c$ is approached. This indicates that, either in the clean or dirty limit, there is no divergence of $m^*$ as the pressure approaches $P_c$.

We now address the issue of the NFL behavior. Figure 6(a) shows the $T$ dependence of $\rho$ under zero field in $EuFe_2As_2$ ($RRR = 13$) at several pressures. Solid curves are fits to $\rho = \rho_0 + CT^x$ ($C$ is a constant). To avoid the effect of $Eu^{2+}$ moments or superconductivity, we use data in a fitting range from 35 K (fixed) to several temperatures between 50 K and $T_0$. Figure 6(b) indicates the $P$ evolution of the exponent $x$. At $P \ll P_c$, Fermi liquid (FL) like behavior ($x \sim 2$) is observed. As the pressure approaches $P_c$, $x$ decreases rapidly and reaches approximately unity.

It has previously been proposed that the $T$-linear resistivity in iron-based SCs arises from the $T$-dependent carrier concentration and that the carrier scattering rate $\tau^{-1}$ obeys a standard FL $T^2$ law.[24,25] We therefore show the $T$ dependence of $(m^*/m_0)/\tau_i = (e/m_0)\mu_i^{-1}$ at 2.9, 3.1, and 3.2 GPa ($>P_c$) obtained from the above two-carrier analyses in Fig. 7. The figures indicate that the scattering rates for both electrons and holes are nearly proportional to $T$ in a remarkably wide $T$ range. Although we have assumed

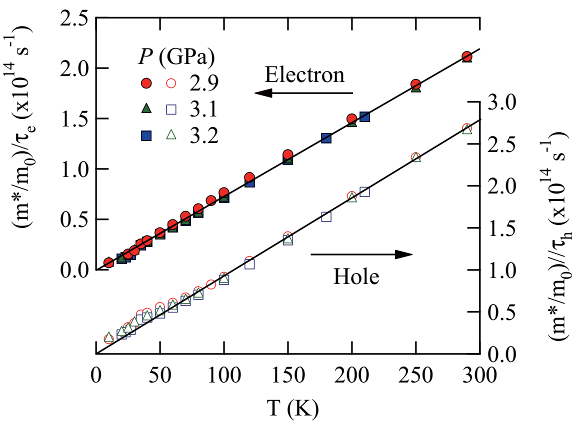


FIG. 7. (Color online) $(m^*/m_0)/\tau_i$ vs $T$ for electron ($i$ = E) and hole ($i$ = H) at 2.9, 3.1, and 3.2 GPa ($>P_c$). Solid lines are a guide to the eyes.

$n_H = n_E = 7.5 \times 10^{-2}$ e/Fe in estimating $\mu_i$ as noted above, any carrier number in the range between 0.05 and 0.1 e/Fe gives a similar approximately $T$-linear dependence of $\mu_i$.

Figure 8 shows $\rho(T)$ at 2.9 GPa ($\sim P_c$) under several fields of up to 15 T. The FL $T^2$ behavior is gradually restored with increasing $B$. To estimate the $T$ variation of the exponent $x$ under applied fields, we fit the data to $\rho = \rho_0 + CT^x$ in several temperature ranges. The inset of Fig. 8 shows the $T$ variation of $x$ under 0, 8, and 15 T. Under zero field, the $x$ value is close to one. Under applied fields of 8 and 15 T, with decreasing $T$, the $x$ value increases from $\sim$1 and approaches $\sim$2. This clearly indicates that the origin of the $T$-linear resistivity is spin fluctuations. As is well known, spin fluctuation theories predict $T$-linear resistivity for two-dimensional nearly AF metals.[49] To our knowledge, there has been no observation of a $B$-induced change in the resistivity exponent from 1 to 2 in iron-based SCs. The present observation is most likely to result from the fact that the conduction carrier spins are influenced by the large exchange field from the $Eu^{2+}$ moments, in addition to the externally applied field. That is, as soon as the $Eu^{2+}$ moments are fully aligned by the applied field, the conduction electrons feel a large exchange field of $-B_J^m = -75$ T, which effectively suppresses the spin fluctuations.

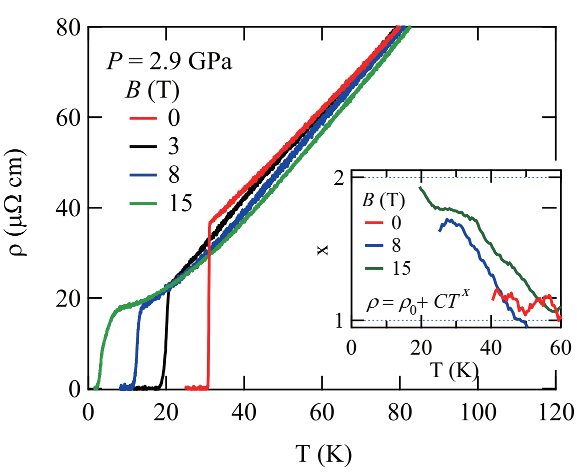


FIG. 8. (Color online) $\rho(T)$ at 2.9 GPa under 0, 3, 8, and 15 T. The inset shows the $T$ dependence of $x$ under several fields.

## IV. CONCLUSIONS

To conclude, our analyses of magnetotransport and upper critical fields in $EuFe_2As_2$ under high pressure indicate that there is no QCP at $P_c$ in this pure compound, which is in sharp contrast to the observation in $BaFe_2(As,P)_2$.[19,50] On the other hand, we have shown that the scattering rates for both electrons and holes are approximately $T$-linear for $P > P_c$. The recovery of the FL $T^2$ dependence of $\rho$ at high fields clearly indicates that spin fluctuations are the origin of the anomalous scattering. It appears that systematic analyses of spin (and/or orbital) fluctuations based on the electronic structures of individual materials, beyond a generic scenario based on a QCP, are necessary to elucidate the mechanism of iron-based superconductivity.

## ACKNOWLEDGMENT

We would like to thank H. Eisaki, S. Ishida, and H. Harima for fruitful discussions. This work was partially supported by a Grant-in-Aid for Young Scientists (No. 23740279) from the Ministry of Education, Culture, Sports, Science and Technology, Japan.

## APPENDIX

The procedure for the three carrier analysis used in simultaneously fitting the obtained $\rho$ and $\rho_H$ data of $EuFe_2As_2$ is shown below. This procedure is essentially the same as that used in the recent work on the sister compound $BaFe_2As_2$.[44]

Tensor components of the electrical conductivity, $\sigma_{xx}$ ($=\sigma_{yy}$) and $\sigma_{xy}$ ($=-\sigma_{yx}$), for three carriers can be expressed in the following forms using those of the electrical resistivity, $\rho_{xx}$ ($=\rho_{yy}=\rho$) and $\rho_{xy}$ ($=-\rho_{yx}=\rho_H$):

$$\begin{aligned}\sigma_{xx} &= \frac{\rho_{xx}}{\rho_{xx}^2+\rho_{xy}^2} = \sum_{i=1}^{3}\frac{q_i n_i \mu_i}{1+(\mu_i B)^2},\\ \sigma_{xy} &= \frac{\rho_{xy}}{\rho_{xx}^2+\rho_{xy}^2} = \sum_{i=1}^{3}\frac{q_i n_i \mu_i^2 B}{1+(\mu_i B)^2},\end{aligned} \tag{A1}$$

where $q_i$, $n_i$, and $\mu_i$ are the charge, density, and mobility of the $i$th carrier, respectively, and the tensors of the electrical conductivity $\boldsymbol{\sigma}$ and resistivity $\boldsymbol{\rho}$ have the forms

$$\boldsymbol{\sigma} = \begin{pmatrix}\sigma_{xx} & \sigma_{xy}\\ -\sigma_{xy} & \sigma_{xx}\end{pmatrix}, \quad \boldsymbol{\rho} = \begin{pmatrix}\rho_{xx} & \rho_{xy}\\ -\rho_{xy} & \rho_{xx}\end{pmatrix}. \tag{A2}$$

From Eq. (1), $\rho_{xx}$ and $\rho_{xy}$ can be written as follows:

$$\begin{aligned}\rho_{xx} &= \frac{\sum_{i=1}^{3}\frac{q_i n_i \mu_i}{1+(\mu_i B)^2}}{\sum_{i=1}^{3}\frac{q_i n_i \mu_i}{1+(\mu_i B)^2}+\sum_{i=1}^{3}\frac{q_i n_i \mu_i^2 B}{1+(\mu_i B)^2}},\\ \rho_{xy} &= \frac{\sum_{i=1}^{3}\frac{q_i n_i \mu_i^2 B}{1+(\mu_i B)^2}}{\sum_{i=1}^{3}\frac{q_i n_i \mu_i}{1+(\mu_i B)^2}+\sum_{i=1}^{3}\frac{q_i n_i \mu_i^2 B}{1+(\mu_i B)^2}}.\end{aligned} \tag{A3}$$

*Present address: Department of Physics, Tokyo Institute of Technology, Meguro-ku, Tokyo 152-8551, Japan.

[1] Y. Kamihara, T. Watanabe, M. Hirano, and H. Hosono, J. Am. Chem. Soc. **130**, 3296 (2008).
[2] For recent reviews, see D. C. Johnston, Adv. Phys. **59**, 803 (2010); G. R. Stewart, Rev. Mod. Phys. **83**, 1589 (2011).
[3] H. Kito, H. Eisaki, and A. Iyo, J. Phys. Soc. Jpn. **77**, 063707 (2008).
[4] Z.-A. Ren, W. Lu, J. Yang, W. Yi, X.-L. Shen, Z.-C. Li, G.-C. Che, X.-L. Dong, L.-L. Sun, F. Zhou, and Z.-X. Zhou, Chin. Phys. Lett. **25**, 2215 (2008).
[5] C. Wang, L. Li, S. Chi, Z. Zhu, Z. Ren, Y. Li, Y. Wang, X. Lin, Y. Luo, S. Jiang, X. Xu, G. Cao, and Z. Xu, Europhys. Lett. **83**, 67006 (2008).
[6] M. Rotter, M. Tegel, and D. Johrendt, Phys. Rev. Lett. **101**, 107006 (2008).
[7] I. I. Mazin, D. J. Singh, M. D. Johannes, and M. H. Du, Phys. Rev. Lett. **101**, 057003 (2008).
[8] K. Kuroki, H. Usui, S. Onari, R. Arita, and H. Aoki, Phys. Rev. B **79**, 224511 (2009).
[9] Y. Nakai, K. Ishida, Y. Kamihara, M. Hirano, and H. Hosono, J. Phys. Soc. Jpn. **77**, 073701 (2008).
[10] K. Hashimoto, M. Yamashita, S. Kasahara, Y. Senshu, N. Nakata, S. Tonegawa, K. Ikada, A. Serafin, A. Carrington, T. Terashima, H. Ikeda, T. Shibauchi, and Y. Matsuda, Phys. Rev. B **81**, 220501(R) (2010).
[11] H. Kontani and S. Onari, Phys. Rev. Lett. **104**, 157001 (2010).
[12] M. Sato, Y. Kobayashi, S. C. Lee, H. Takahashi, E. Satomi, and Y. Miura, J. Phys. Soc. Jpn. **79**, 014710 (2010).
[13] D. J. Singh and M.-H. Du, Phys. Rev. Lett. **100**, 237003 (2008).
[14] H. Ding, P. Richard, K. Nakayama, K. Sugawara, T. Arakane, Y. Sekiba, A. Takayama, S. Souma, T. Sato, T. Takahashi, Z. Wang, X. Dai, Z. Fang, G. F. Chen, J. L. Luo, and N. L. Wang, Eur. Phys. Lett. **83**, 47001 (2008).
[15] P. L. Alireza, J. Gillett, Y. T. Chris Ko, S. E. Sebastian, and G. G. Lonzarich, J. Phys.: Condens. Matter **21**, 012208 (2009).
[16] R. H. Liu, G. Wu, T. Wu, D. F. Fang, H. Chen, S. Y. Li, K. Liu, Y. L. Xie, X. F. Wang, R. L. Yang, L. Ding, C. He, D. L. Feng, and X. H. Chen, Phys. Rev. Lett. **101**, 087001 (2008).
[17] M. Gooch, B. Lv, B. Lorenz, A. M. Guloy, and C.-W. Chu, Phys. Rev. B **79**, 104504 (2009).
[18] J. Dai, Q. Si, J. -X. Zhu, and E. Abrahams, Proc. Natl. Acad. Sci. USA, **106**, 4118 (2009).
[19] K. Hashimoto, K. Cho, T. Shibauchi, S. Kasahara, Y. Mizukami, R. Katsumata, Y. Tsuruhara, T. Terashima, H. Ikeda, M. A. Tanatar, H. Kitano, N. Salovich, R. W. Giannetta, P. Walmsley, A. Carrington, R. Prozorov, and Y. Matsuda, Science **336**, 1554 (2012).
[20] H. Luetkens, H.-H. Klauss, M. Kraken, F. J. Litterst, T. Dellmann, R. Klingeler, C. Hess, R. Khasanov, A. Amato, C. Baines, M. Kosmala, O. J. Schumann, M. Braden, J. Hamann-Borrero, N. Leps, A. Kondrat, G. Behr, J. Werner, and B. Büchner, Nat. Mater. **8**, 305 (2009).
[21] S. Iimura, S. Matuishi, H. Sato, T. Hanna, Y. Muraba, S. W. Kim, J. E. Kim, M. Takata, and H. Hosono, Nat. Commun. **3**, 943 (2012).
[22] M. Nakajima, S. Ishida, K. Kihou, Y. Tomioka, T. Ito, Y. Yoshida, C. H. Lee, H. Kito, A. Iyo, H. Eisaki, K. M. Kojima, and S. Uchida, Phys. Rev. B **81**, 104528 (2010).
[23] R. T. Gordon, H. Kim, N. Salovich, R. W. Giannetta, R. M. Fernandes, V. G. Kogan, T. Prozorov, S. L. Bud'ko, P. C. Canfield, M. A. Tanatar, and R. Prozorov, Phys. Rev. B **82**, 054507 (2010).
[24] L. Fang, H. Luo, P. Cheng, Z. Wang, Y. Jia, G. Mu, B. Shen, I. I. Mazin, L. Shan, C. Ren, and H.-H. Wen, Phys. Rev. B **80**, 140508(R) (2009).
[25] F. Rullier-Albenque, D. Colson, A. Forget, and H. Alloul, Phys. Rev. Lett. **103**, 057001 (2009).
[26] C. F. Miclea, M. Nicklas, H. S. Jeevan, D. Kasinathan, Z. Hossain, H. Rosner, P. Gegenwart, C. Geibel, and F. Steglich, Phys. Rev. B **79**, 212509 (2009).
[27] T. Terashima, M. Kimata, H. Satsukawa, A. Harada, K. Hazama, S. Uji, H. S. Suzuki, T. Matsumoto, and K. Murata, J. Phys. Soc. Jpn. **78**, 083701 (2009); **78**, 118001 (2009.
[28] N. Kurita, M. Kimata, K. Kodama, A. Harada, M. Tomita, H. S. Suzuki, T. Matsumoto, K. Murata, S. Uji, and T. Terashima, J. Phys.: Conf. Ser. **273**, 012098 (2011).
[29] N. Kurita, M. Kimata, K. Kodama, A. Harada, M. Tomita, H. S. Suzuki, T. Matsumoto, K. Murata, S. Uji, and T. Terashima, Phys. Rev. B **83**, 214513 (2011).
[30] K. Matsubayashi, K. Munakata, M. Isobe, N. Katayama, K. Ohgushi,Y. Ueda, Y. Uwatoko, N. Kawamura, M. Mizumaki, N. Ishimatsu, M. Hedo, and I. Umehara, Phys. Rev. B **84**, 024502 (2011).
[31] S. Jiang, Y. Luo, Z. Ren, Z. Zhu, C. Wang, X. Xu, Q. Tao, G. Cao, and Z. Xu, New J. Phys. **11**, 025007 (2009).
[32] Y. Xiao, Y. Su, M. Meven, R. Mittal, C. M. N. Kumar, T. Chatterji, S. Price, J. Persson, N. Kumar, S. K. Dhar, A. Thamizhavel, and Th. Brueckel, Phys. Rev. B **80**, 174424 (2009).
[33] Y. Xiao, Y. Su, W. Schmidt, K. Schmalzl, C. M. N. Kumar, S. Price, T. Chatterji, R. Mittal, L. J. Chang, S. Nandi, N. Kumar, S. K. Dhar, A. Thamizhavel, and Th. Brueckel, Phys. Rev. B **81**, 220406(R) (2010).
[34] T. Terashima, N. Kurita, A. Kikkawa, H. S. Suzuki, T. Matsumoto, K. Murata, and S. Uji, J. Phys. Soc. Jpn. **79**, 103706 (2010).
[35] N. Kurita, M. Kimata, K. Kodama, A. Harada, M. Tomita, H. S. Suzuki, T. Matsumoto, K. Murata, S. Uji, and T. Terashima, Phys. Rev. B **83**, 100501(R) (2011).
[36] F. Hunte, J. Jaroszynski, A. Gurevich, D. C. Larbalestier, R. Jin, A. S. Sefat, M. A. McGuire, B. C. Sales, D. K. Christen, and D. Mandrus, Nature (London) **453**, 903 (2008).
[37] H. Q. Yuan, J. Singleton, F. F. Balakirev, S. A. Baily, G. F. Chen, J. L. Luo, and N. L. Wang, Nature (London) **457**, 565 (2009).
[38] H. Kotegawa, H. Sugawara, and H. Tou, J. Phys. Soc. Jpn. **78**, 013709 (2009).
[39] Y. Uwatoko, M. Hedo, N. Kurita, M. Koeda, M. Abliz, and T. Matsumoto Physica C **329–333**, 1658 (2003).
[40] K. Murata, K. Yokogawa, H. Yoshino, S. Klotz, P. Munsch, A. Irizawa, M. Nishiyama, K. Iizuka, T. Nanba, T. Okada, Y. Shiraga, and S. Aoyama, Rev. Sci. Instrum. **79**, 085101 (2008).
[41] $R_H(T)$ estimated at different $B$ shows qualitatively similar behavior.
[42] S. Kasahara, T. Shibauchi, K. Hashimoto, K. Ikada, S. Tonegawa, R. Okazaki, H. Shishido, H. Ikeda, H. Takeya, K. Hirata, T. Terashima, and Y. Matsuda, Phys. Rev. B **81**, 184519 (2010).
[43] T. Terashima, N. Kurita, M. Tomita, K. Kihou, C.-H. Lee, Y. Tomioka, T. Ito, A. Iyo, H. Eisaki, T. Liang, M. Nakajima, S. Ishida, S.-i. Uchida, H. Harima, and S. Uji, Phys. Rev. Lett. **107**, 176402 (2011).

[44] S. Ishida, T. Liang, M. Nakajima, K. Kihou, C. H. Lee, A. Iyo, H. Eisaki, T. Kakeshita, T. Kida, M. Hagiwara, Y. Tomioka, T. Ito, and S. Uchida, Phys. Rev. B **84**, 184514 (2011).

[45] H. Shishido, A. F. Bangura, A. I. Coldea, S. Tonegawa, K. Hashimoto, S. Kasahara, P. M. C. Rourke, H. Ikeda, T. Terashima, R. Settai, Y. Onuki, D. Vignolles, C. Proust, B. Vignolle, A. McCollam, Y. Matsuda, T. Shibauchi, and A. Carrington, Phys. Rev. Lett. **104**, 057008 (2010).

[46] L. Ortenzi, E. Cappelluti, L. Benfatto, and L. Pietronero, Phys. Rev. Lett. **103**, 046404 (2009).

[47] N. R. Werthamer, E. Helfand, and P. C. Hohenberg, Phys. Rev. **147**, 295 (1966).

[48] Ø. Fischer, Helv. Phys. Acta **45**, 331 (1972).

[49] T. Moriya, Y. Takahashi, and K. Ueda, J. Phys. Soc. Jpn. **59**, 2905 (1990).

[50] P. Walmsley, C. Putzke, L. Malone, I. Guillamón, D. Vignolles, C. Proust, S. Badoux, A. I. Coldea, M. D. Watson, S. Kasahara, Y. Mizukami, T. Shibauchi, Y. Matsuda, and A. Carrington, Phys. Rev. Lett. **110**, 257002 (2013).